

Article

Study on the Basic Performance Deterioration Law and the Application of Lead Rubber Bearings under the Alternation of Aging and Seawater Erosion

Yanmin Li ^{1,2,3}, Yuhong Ma ^{1,2,3,*}, Guifeng Zhao ^{2,4,*} and Rong Liu ¹

- ¹ Earthquake Engineering Research & Test Center, Guangzhou University, Guangzhou 510006, China
² Guangdong Key Laboratory of Earthquake Engineering & Applied Technique, Guangzhou 510006, China
³ Key Laboratory of Earthquake Resistance, Earthquake Mitigation and Structural Safety, Ministry of Education, Guangzhou 510006, China
⁴ School of Civil Engineering, Guangzhou University, Guangzhou 510006, China
* Correspondence: myhzth@gzhu.edu.cn (Y.M.); zgfzth@gzhu.edu.cn (G.Z.); Tel.: +86-020-86395101 (Y.M.)

Abstract: Lead rubber isolation bearings are well-recognized as a common and effective means to mitigate the seismic responses of bridges. However, rubber isolation bearings used in offshore bridges are extremely vulnerable to the action of the alternation of aging and seawater erosion caused by weather conditions, wind, waves, and other factors. Meanwhile, the deterioration law and application of lead rubber bearings subject to the effect of aging and seawater erosion cycles are not clear. Thus, aging and seawater erosion cycles testing on both lead rubber isolation bearings (LRB) and rubber materials were carried out. The parameters for the Mooney–Rivlin model of the rubber material used in LRBs were determined and the time-varying law of basic performance of LRBs was obtained based on test results of LRBs and their rubber material. Then, the determined rubber material parameters were applied into the finite-element model of LRBs to verify the basic performance degradation law of the LRBs. Finally, the obtained basic performance degradation law of LRBs was substituted into the finite model of offshore bridges to investigate the impact of the property degradation of LRBs on their seismic performance. The time-varying law of seismic performance of offshore bridge structures was also studied based on finite element analysis. The results show that both the horizontal and vertical stiffness of LRBs increase with the alternating of aging and seawater erosion time, and the horizontal and vertical stiffness increase by 16.1% and 24.3%, respectively, during the 120-year service period. Additionally, the Mooney–Rivlin model parameters of the LRB rubber material are also significantly affected by the alternating of aging and seawater erosion. Additionally, the results also indicate the deterioration of LRBs has a great influence on the anti-seismic performance of offshore bridge structures. After 120 years of service of offshore bridge isolation bearings under the alternating of aging and seawater erosion, the maximum displacement of the pier top of the offshore bridges, the maximum bending moment at the pier bottom, and the maximum displacement of the rubber bearing increased by 14.2%, 6.6%, and 9.1%, respectively. The findings of this paper play an important role in the seismic behavior study and the life-cycle performance analysis of offshore traffic projects such as sea-crossing bridges in marine environments. At the same time, they also lay a theoretical foundation for the performance analysis of rubber isolation bearings and offshore bridge structures under the alternation of aging and seawater erosion cycles.



Citation: Li, Y.; Ma, Y.; Zhao, G.; Liu, R. Study on the Basic Performance Deterioration Law and the Application of Lead Rubber Bearings under the Alternation of Aging and Seawater Erosion. *Buildings* **2023**, *13*, 360. <https://doi.org/10.3390/buildings13020360>

Academic Editor: Fabrizio Greco

Received: 19 December 2022

Revised: 16 January 2023

Accepted: 18 January 2023

Published: 28 January 2023



Copyright: © 2023 by the authors. Licensee MDPI, Basel, Switzerland. This article is an open access article distributed under the terms and conditions of the Creative Commons Attribution (CC BY) license (<https://creativecommons.org/licenses/by/4.0/>).

Keywords: alternation of aging and seawater erosion; lead rubber isolation bearing; basic performance; deterioration law; offshore bridge; seismic performance

1. Introduction

In recent years, the construction of offshore transportation engineering such as sea-crossing bridges has become increasingly prosperous. More and more sea-crossing bridges have adopted the relatively mature rubber isolation technology, such as the Hong Kong

Zhuhai Macao Bridge opened in 2019. Natural rubber isolation bearings (LNR), high damping rubber isolation bearings (HDR) and lead rubber isolation bearings (LRB) are the most commonly used rubber bearings in bridge isolation. Among them, lead rubber bearings are the most widely used. In view of the long coastline of China, and because rubber isolation bearings for sea-crossing bridges will remain in challenging ocean environment for the long term, they are easily subjected to the aging and seawater erosion cycles caused by factors such as weather, rain, waves, tides, wind, and so on. This effect mentioned above may lead to the deterioration or even failure of rubber isolation bearings, which may threaten the seismic safety of offshore bridges or sea-crossing bridge structures. Therefore, exploring degradation laws and the application of lead rubber isolation bearings under the aging and seawater erosion cycles plays an important role in the decision making and performance evaluating of the isolation scheme for offshore bridges.

At present, there are many reports on the basic performance and aging performance of rubber bearings at home and abroad, but there are few reports on the basic performance and application of lead rubber isolation bearings under the alternating action of aging and seawater erosion. Both systematic experimental research on the mechanical properties of bridge high damping bearings and comparative tests on the mechanical properties of the rubber bearings of different bridges have been conducted by Shen Chaoyong et al. [1,2], and the fitting empirical formulas for the mechanical properties of HDRs and LRBs were given in the two papers. Akihiro [3] studied the mechanical behavior of rubber bearings through finite element analysis and put forward an evaluation method for natural rubber bearings' mechanical performance. A comparative test on the accelerated deterioration of laminated rubber isolation bearings and rubber sheets has been conducted by Xu Bin et al. [4], and the change law of horizontal stiffness was obtained after 80 years of service at 20 °C ambient temperature. Y Itoh et al. [5–9] carried out a series of experiments on natural rubber bearings, high damping rubber bearings, and rubber materials; they also predicted the performance degradation model of high damping rubber bearings and analyzed the internal aging law of natural rubber bearings. Wang Jianqiang et al. [10,11] studied the impact of compression stress and shear strains on the shear properties of HDRs and LRBs at room temperature, and then put forward the empirical formula for the correlation between the shear performance of HDRs and LRBs and shear strain and compressive stress. In order to reduce the seismic excitations of bridge structures, Li et al. [12] designed and processed a high damping rubber bearing and studied its mechanical properties. The research results provide a basis for the shaking table test of a continuous beam bridge with high damping rubber isolation bearings. Accelerated-aging tests and finite element simulation on lead rubber bearings were conducted by J. Park et al. [13], and the aging performance coefficient of lead rubber bearings was also studied. Kalpakidis V. I. et al. [14,15] proposed a theoretical method to predict the characteristic strength and dissipation capacity of lead rubber bearing over time. Takenaka Y. et al. [16] studied the thermo-mechanical interaction effect of the laminated rubber bearings under larger and more cyclic lateral movement, and then conducted dynamic tests on full-size and scaled rubber bearing specimens under sinusoidal and seismic response displacement input to verify their damping characteristics when affected by temperature rise.

In addition, the present research on the seismic behavior of offshore bridges is mostly concentrated on the seismic performance of bridge structures or main components under the condition of pier deterioration and material deterioration. The probabilistic time-varying nonlinear static analysis method of structural systems was used by Biondini [17] to investigate the seismic performance of bridge structures based on the randomness of erosion processes and the uncertainty of material and geometry. Alipour et al. [18] studied the probability of seismic risk considering chloride ion corrosion and the degree of structural degradation during the service period for reinforced concrete highway bridges. Kobayashi et al. [19] studied the seismic performance degradation of reinforced concrete beams under chloride ion erosion environment. Choe et al. [20] investigated the impact of performance degradation of reinforcement materials on the seismic performance of bridges. The results

showed that the corrosion of reinforcement materials reduces the seismic performance of bridge structures. Gosh J. et al. [21] conducted a vulnerability study of bridge structures under the condition of corrosion of the bearings and pier reinforcement materials. Zhao Guifeng et al. [22] studied the seismic performance of Hong Kong Zhuhai Macao Bridge in the whole service life under the condition of deterioration of the friction pendulum bearings. Chen Jiajia et al. [23] carried out the research on the time-varying vulnerability of offshore isolated bridges based on the aging time-varying law of natural rubber bearings. Farhangi and Karakouzian [24] studied the structural responses of glass-fiber-reinforced polymer (GFRP) tubes filled with regenerated concrete material to develop compound piles, and which can be used as a substitute for traditional steel reinforced piles in bridge foundations. They additionally indicated that, according to the curve interaction diagram, the combination of pipe wall thickness and GFRP fiber content can meet the required axial and flexural bearing capacity of piles in different eccentricity ranges. Additionally, a new anti-seismic abutment with high-capacity wing walls was presented and analytically studied by Mitoulis et al. [25], and the earthquake-resistant behavior of the proposed anti-seismic abutment was evaluated by utilizing a benchmark bridge. The results showed that the proposed unconventional design is reliable. Nutt et al. [26] used AASHTO division I-A to compare the typical bridge columns with and without abutment in seismic design and raised AASHTO LRFD provisions.

To sum up, most of the comparative studies on bearing performance do not consider the influence of the marine environment, and most of the durability studies focus on aging performance. There are few studies on the time-varying law of the performance degradation of rubber isolation bearings and few reports on the influence of the marine environment such as the effect of aging and seawater erosion cycles or marine erosion on the performance of bridge rubber bearings. Comparative study on the degradation of lead rubber isolation bearings is rarer. Now, the influence of performance degradation of lead rubber bearings on the seismic performance of bridge structure is not clear. In order to study the influence of the alternating of aging and seawater erosion on the performance degradation law of lead rubber isolation bearings and the time-dependent law of seismic performance of offshore isolation bridges under the condition of bearing degradation, the research group carried out a seawater dry-wet cycle test and an aging and seawater erosion test of bridge natural rubber bearings, high damping rubber isolation bearings, and their rubber materials [27–30], and the change law of rubber material and bearing performance was also revealed in references [27–30]. In this paper, an age and seawater corrosion alternating test on LRBs and their rubber materials was carried out, and the time-dependent law of LRB rubber material parameters was fitted and calculated according to the relevant data. Then, this was verified by the finite-element analytical method, and the time-variable law of the horizontal and vertical stiffness ratio of lead rubber isolation bearings under aging and seawater erosion cycles is summarized. Finally, the time-varying rule of seismic performance of an offshore isolation bridge was analyzed based on the performance degradation law of lead rubber bearings. The research results provide a good theoretical basis for seismic isolation design, life-cycle seismic performance evaluation, and the usage and maintenance of cross-sea bridges and other ocean engineering in future, and can also provide a theoretical basis for exploring the impact of bridge support performance degradation on the full life-cycle seismic behavior of marine engineering structures such as cross-sea bridges. It is of great significance for us to better understand the performance degradation of rubber isolation bearings and the deterioration law of the structural performance of isolated bridges in marine environments.

2. Overview of the Age and Seawater Alternating Corrosion Test on Lead Rubber Bearings

Considering the weather ratio of the top ten coastal cities in China and the possibility of the alternation of aging and seawater corrosion caused by sea breeze, sea wave, sea tide, and so on [27,29], the research group carried out an aging and seawater corrosion

cycles test on natural rubber isolation bearings, high damping rubber bearings, and their rubber materials. The aging and seawater corrosion cycles test was carried out on the lead rubber bearing and its rubber material in this paper, to investigate the performance deterioration law of LRBs and their rubber material and to also explore its influence on the seismic performance of offshore bridge structures. This can lay a foundation for a more systematic understanding of the deterioration law of the performance of different bridge isolation bearings under the alternation of aging and seawater corrosion. The parameters of LRBs, test parameters, and working conditions are shown in Tables 1 and 2. The layout of test samples is shown in Figure 1. The sketch of the bearing and the photograph of the location in the actual structure are shown in Figures 2 and 3.



Figure 1. Sample placement diagram. (a) Soaking in seawater; (b) drying in an aging tank.

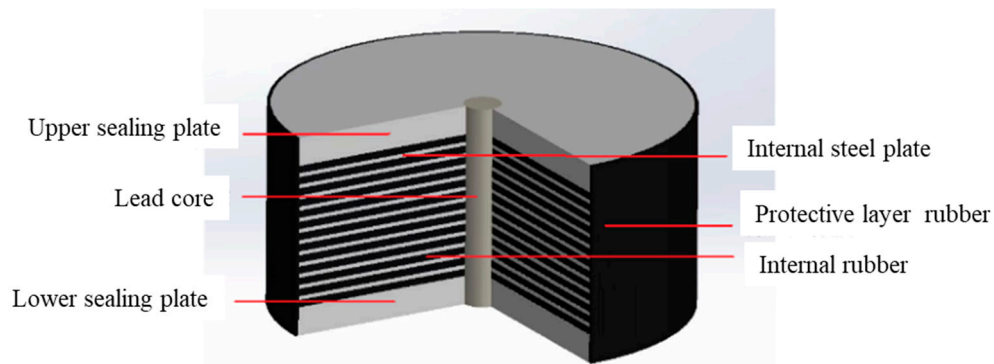


Figure 2. Sketch of an LRB.

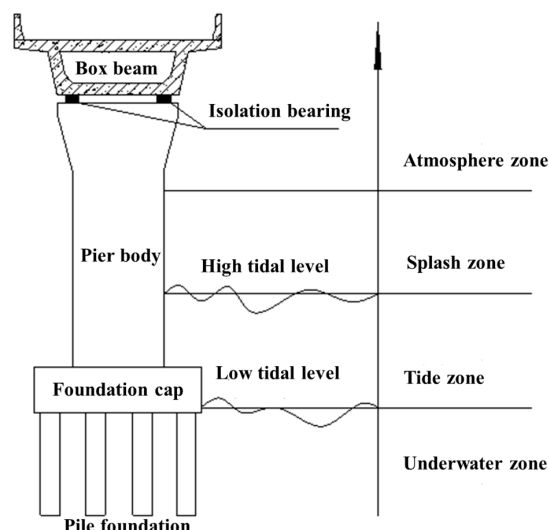


Figure 3. The photograph of the location in the actual structure.

Table 1. Parameters of LRBs.

Test Specimen	Shear Modulus (MPa)	Diameter of Rubber Bearings (mm)	Thickness of Cover Steel Plate (mm)	Thickness of Single Inner Rubber (mm)	Number of Layers of Inner Rubber	Thickness of Inner Steel Plate (mm)	Number of Inner Steel Plates	Total Thickness of Rubber Layers (mm)	Bearing Height (mm)	First Shape Factor S1	Second Shape Factor S2
LRB	0.8	220	20	5.3	8	3	7	42.4	103.4	8.96	5.2

Table 2. Test parameters and working conditions.

Test Body and Its Number	Total Test Time (days)	Speedup Ratio of Test	Equivalent to the Actual Service Time (years)	Test Temperature (°C)	Equivalent to the Actual Service Environment Temperature (°C)	Time Ratio of Drying and Soaking	Test Method	Sampling Method	Test Content
LRB21#–LRB25#	120	376	120	80	20	2:1	(a) Specimens were first soaked for one day in artificial seawater in the aging box at 80 °C. (b) Then, the specimens were dried for two days in aging box at 80 °C without artificial seawater. (c) Above cycle test was carried out until the end of the 120-day test.	Specimens LRB21#–LRB25# were sampled at 0, 15, 30, 45, 60, 90, 105, and 120 days, respectively.	(1) Horizontal stiffness; (2) Vertical stiffness.

It can be seen from Table 2 that one test day on an LRB is approximately equivalent to its service in the actual environment for one year. Therefore, test time (days) in this paper can be directly converted into the actual environment service time (years).

3. Basic Performance Test Results of Lead Rubber Bearings under the Alternation of Aging and Seawater Corrosion

A 120-day alternating test of aging and seawater corrosion for LRBs and their rubber materials were conducted in this paper. The performance of LRBs and their rubber materials were tested termly in the test process, to investigate the time-varying rule of their mechanical properties. The test method and contents of bearing performance are referred to in [31–33], and the horizontal and vertical stiffness of LRBs were tested on a 500-ton tensile-compression-shear comprehensive testing machine; see Figure 4. This laid the foundation for the application of the deterioration law of LRBs. The appearance changes of the LRBs before and after the test are shown in Figure 5. According to the rest results, the variation law of horizontal equivalent stiffness and vertical stiffness is shown in Figure 6.

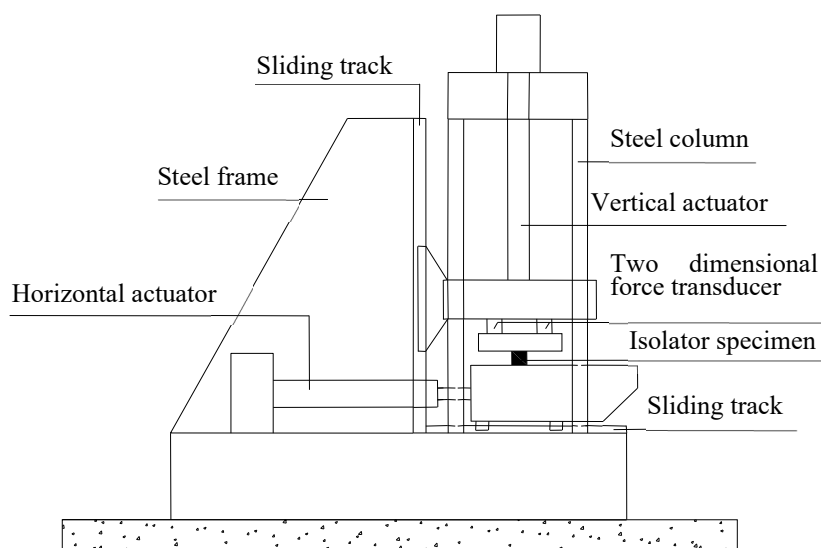


Figure 4. The tension-compression-shear set-up.



Figure 5. Appearance of LRBs before and after testing for 120 days. (a) Day 0; (b) day 120.

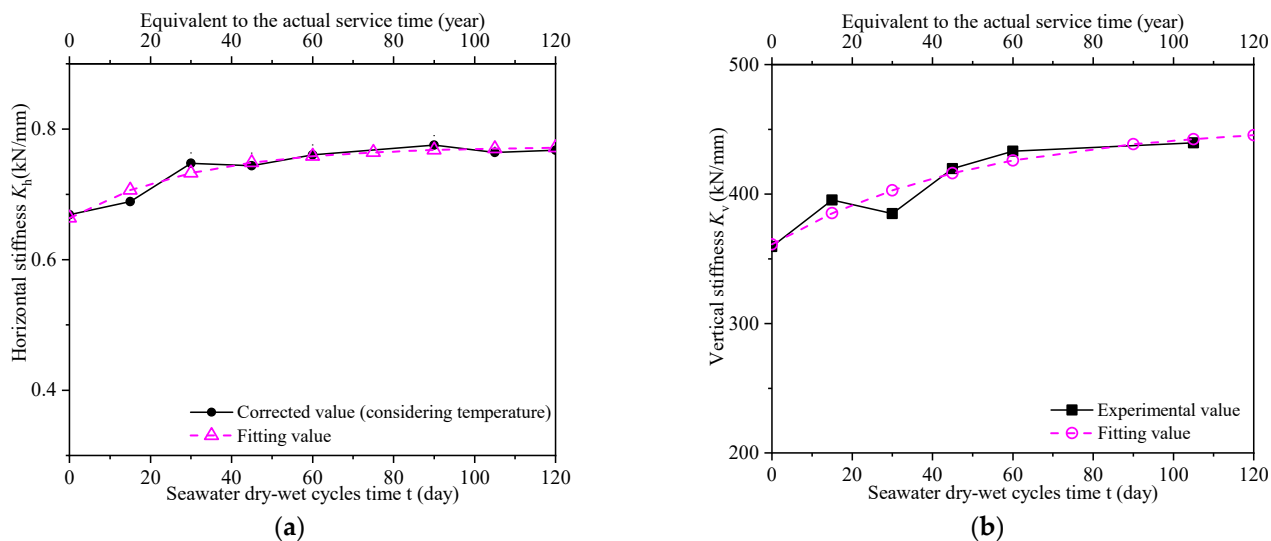


Figure 6. Effect of alternation of aging and seawater corrosion on horizontal and vertical stiffness of LRBs. (a) Horizontal equivalent stiffness; (b) vertical stiffness.

Figure 5 shows that, after testing for 120 days, there was obvious brick red rust and white salt attached to the appearance of the LRBs, and the surface gloss was obviously faded. This indicates that the alternation of aging and seawater corrosion has an important impact on the appearance of LRBs.

Figure 6a shows that the horizontal equivalent stiffness of LRBs increases exponentially with the time of the aging and seawater corrosion alternation test. Figure 6a also indicates that the fitting and test values of the LRBs' horizontal equivalent stiffness coincide with each other well, and the deviation between them both is shown in Table 3. The fitting results state that the horizontal stiffness of LRBs increases exponentially with test time (see Formula (1)). After testing for 60 days (equivalent to an LRB service for 60 years in an actual environment) and 120 days, the growth rates were 14.3% and 16.3%, respectively. Figure 6b indicates that the vertical stiffness of LRBs increases slowly with test time, and the fitting results are in good agreement with the experimental results; deviations between them both are also shown in Table 3. The fitting results also state that the growth amplitudes of vertical stiffness are 18% and 24.3%, respectively, after the LRB testing for 60 days and 120 days.

Table 3. Variation between the fitted value and experimental value of LRB basic performance and its increase (%).

Bearing Type	Horizontal Equivalent Stiffness				Vertical Stiffness			
	Maximum Value	Average Value	Growth from 0 to 60 Years	Growth from 60 to 120 Years	Maximum Value	Average Value	Growth from 0 to 60 Years	Growth from 60 to 120 Years
LRB	2.5	1.1	14.3	2.0	4.7	1.8	18	6.3

$$K_h = 0.7735 - 0.11 \times e^{-0.033 \times t} \quad (1)$$

To sum up, the alternation of aging and seawater corrosion plays an important role in the basic horizontal and vertical stiffness of LRBs. The time-varying law of LRBs' basic performance with test time is shown in Formulas (1) and (2). The results state that the growth of the horizontal and vertical stiffness of LRB is 16.3% and 24.3%, respectively, after years of service in the actual environment where aging and seawater corrosion

alternate. Additionally, the increase of the horizontal and vertical stiffness of LRBs is mainly concentrated in 0 to 60 years of its service life.

$$K_v = 453.87 - 92.76 \times e^{-0.02 \times t} \quad (2)$$

4. Comparison Analysis of the Finite-Element Modelling and Experimental Results for LRB Basic Performance

4.1. Determination of the Constitutive Parameters of the LRB Rubber Material

We had carried out the aging and seawater corrosion alternate test on LNRs and rubber material in an earlier stage and the variation law of the rubber material stress-strain and the Mooney–Rivlin constitutive parameters with test time was obtained [27,33–35]. Similar research methods as above were used to investigate the time-dependent law of the Mooney–Rivlin model parameters C_{10} and C_{01} of LRB rubber material. As we all know, the Mooney–Rivlin model is commonly applied to simulate the mechanical property of most rubber materials with small and medium deformation. The typical strain energy density function is shown in Equation (3) [36]. The time = variable law of the model parameters of LRB rubber material with the time of aging and seawater corrosion alternation is shown in Figure 7 and Formulas (4) and (5). Then, the time-dependent law of the rubber material parameters was applied in a finite model (see Figure 8) to simulate the horizontal and vertical stiffness of LRBs. The finite-element model of LRBs is shown in Figure 6. The finite element analysis of performance of lead rubber isolation bearings did not consider the rotational freedom of the bearings. In addition, because the friction cloth is used to replace the connecting plate in the mechanical behavior test of the rubber bearing, the three degrees of freedom of X, Y and Z of the bottom surface of the bearing are restrained in this study, which can better reflect the real boundary conditions. Finally, the calculated values by Formulas (1) and (2) for horizontal stiffness and vertical stiffness were compared with their simulation results, to verify that the time-varying rule of the LRB's basic performance is true and fair.

$$W = C_{10}(I_1 - 3) + C_{01}(I_2 - 3) + \frac{1}{D_1}(J - 1)^2 \quad (3)$$

where W represents the strain potential energy; I_1 , I_2 are invariants of the deviatoric strain tensor; C_{10} , C_{01} , and D_1 are material parameters, which can be decided through material tests of the rubber; and J is the elastic volume ratio.

$$C_{10} = 1.14 - 0.44 \times e^{-\frac{t}{24.36}} \quad (4)$$

$$C_{01} = -0.67 + 0.27 \times e^{-\frac{t}{26.84}} \quad (5)$$

Figure 7 shows that the constitutive parameter C_{10} increases exponentially with the time of the aging and seawater corrosion alternation test, while parameter C_{01} decreases exponentially with test time. It also states that both the fitting values and calculated values for the material parameters are in good agreement with each other; deviations between them both are shown in Table 4.

Table 4. Deviations between the fitting values and calculated values of the rubber material parameters.

Parameter	Deviation (%)		
	Maximum Value	Minimum Value	Average Value
C_{10}	15.2	0.1	4.7
C_{01}	14.7	0	4.2

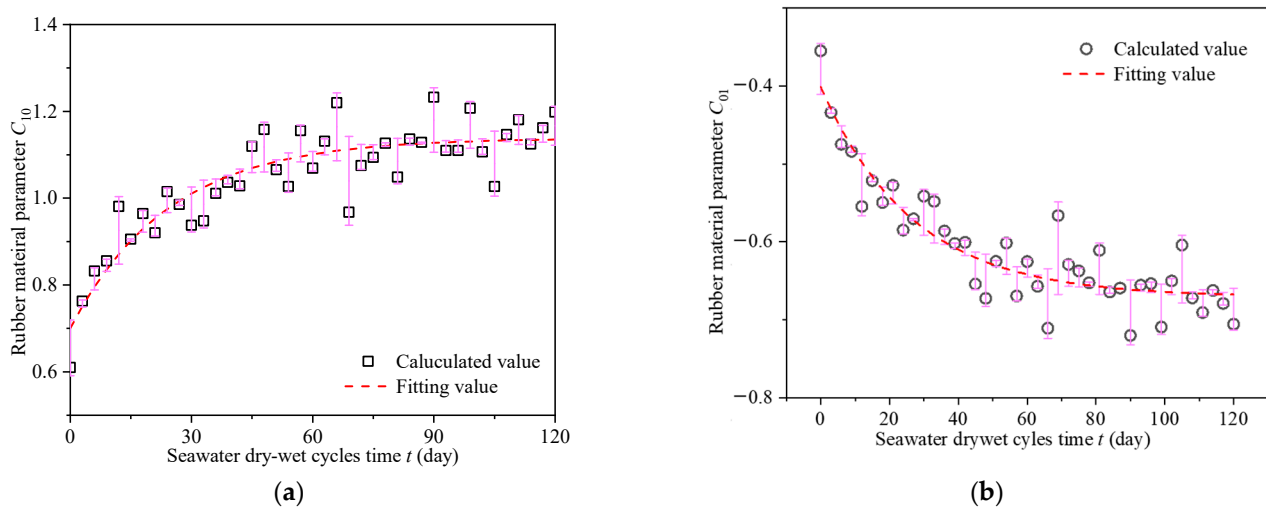


Figure 7. Influence of the alternation of aging and seawater corrosion on LRB rubber material parameters. (a) Material parameter C_{10} ; (b) material parameter C_{01} .

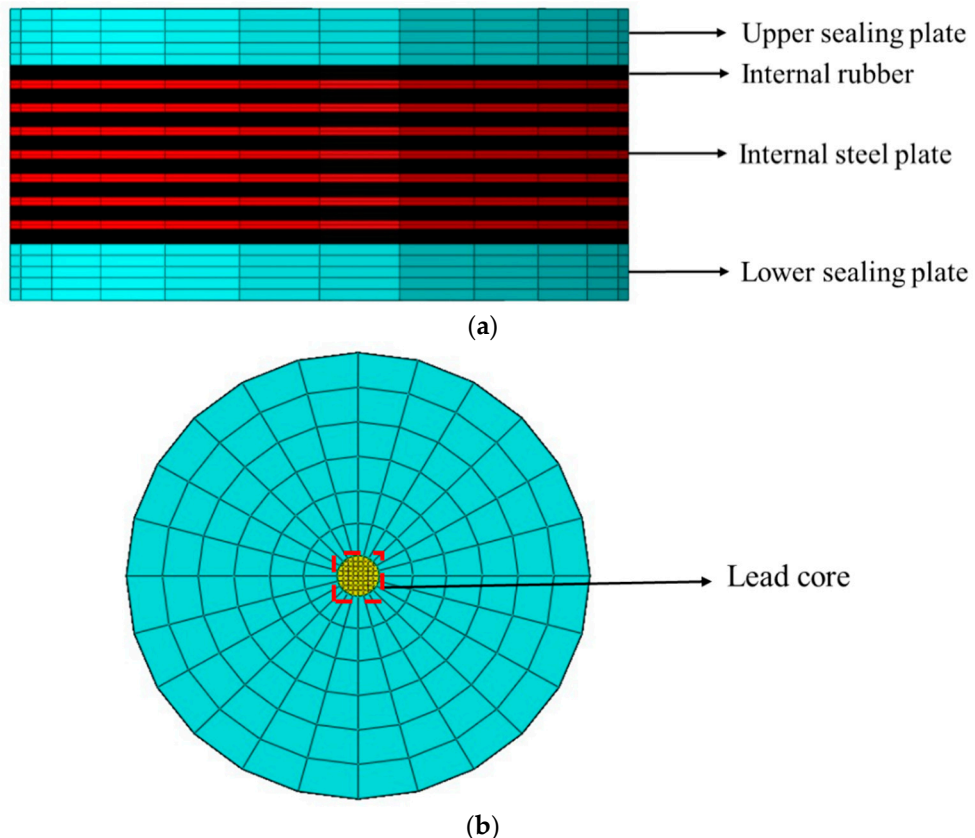


Figure 8. Finite model of the LRB. (a) Side view; (b) vertical view.

4.2. Comparative Analysis of the Simulation and Experimental Results of LRB Basic Performance

This paper used ABAQUS to establish the finite model of LRBs [27], and the LRBs' shape parameters are given in Table 1. The LRB rubber material parameters calculated by Formulas (4) and (5) are applied into the finite model of LRBs to simulate the horizontal and vertical stiffness of LRBs at different test time points. Comparison between the fitting values based on the experimental result in part 2 and the simulation results is shown in Figure 9. Deviation between the above two is shown in Table 5.

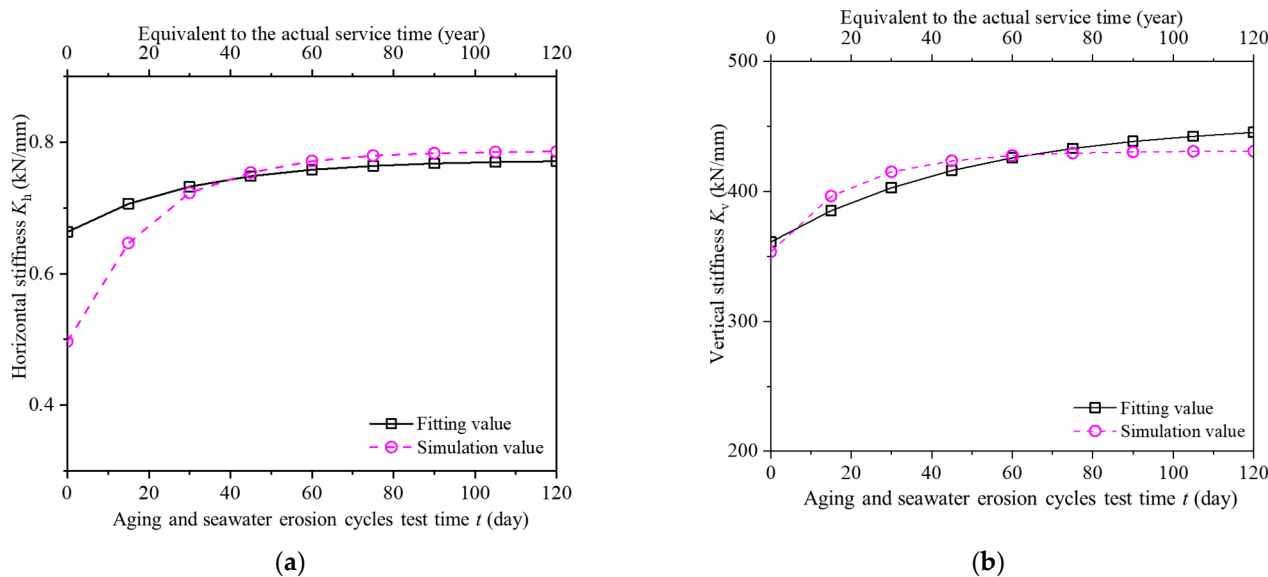


Figure 9. Comparison between finite element simulation values of LRB basic performance and its fitting values. (a) Horizontal equivalent stiffness; (b) vertical stiffness.

Table 5. Deviation between the finite element simulation values of LRB basic performance and its fitting values.

Deviation of Horizontal Equivalent Stiffness (%)			Deviation of Vertical Stiffness (%)		
Maximum	Minimum	Mean	Maximum	Minimum	Mean
25.1	0.7	5	3.2	0.4	2.1

Figure 9 shows that the finite element simulation values of LRB horizontal and vertical stiffness are in good agreement with the fitting values of its test results, and the deviations between the simulation and fitting values are shown in Table 5. This also confirmed that the deterioration law of LRBs' horizontal stiffness and vertical stiffness with the test time, shown in Formulas (1) and (2), is basically accurate.

5. Time-Dependent Law of Seismic Behavior of Isolated Bridges Considering the Performance Degradation of LRBs

5.1. Overview of Isolated Bridges

Sap2000 was used to model an offshore isolated bridge and the seismic response of an offshore bridge considering LRB deterioration alone was analyzed to investigate the influence of LRB deterioration on the time-varying law of seismic performance of offshore bridges. The isolation bridge had a total length of 510 m and was arranged in equal span. Its layout is shown in Figure 10. The main beam of the isolated bridge adopted a steel-concrete composite single-box three-chamber equal section, in which the bridge deck adopted C60 concrete and the box girder adopted a steel truss with a yield strength of about 384 MPa (namely, Q384). The pier was 19 m high and adopted a single-box double-chamber equal-section hollow rectangular section reinforced concrete independent pier, in which the concrete model was C50, and the longitudinal and stirrups used were secondary-thread hot rolled ribbed bars with a yield strength of 335 MPa (namely, HRB335). LRBs were adopted between the main beam and the secondary beam, respectively. Four bearing were arranged on each pier column in parallel. See Table 6 for the relevant parameters of the isolation bearings. The anti-seismic intensity of the isolated bridge was 8 degrees, the site category was grade III, the site characteristic period was 0.65 s, and the design service life was 120 years.

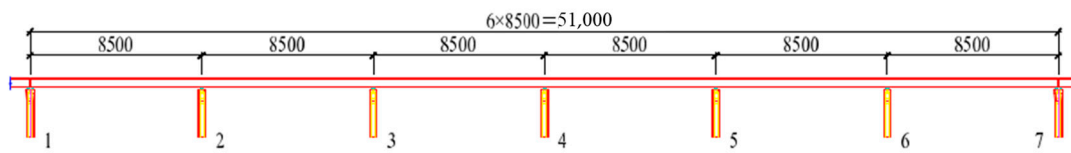


Figure 10. Schematic diagram of the bridge longitudinal structure (unit: cm).

Table 6. Parameters of the LRBs.

Bearing Locations	Bearing Type	Vertical Bearing Capacity (kN)	Yield Force (kN)	Initial Shear Stiffness (kN/mm)	Post-Yielding Stiffness (kn/mm)	Equivalent Horizontal Stiffness (kn/mm)	Vertical Stiffness (kN/mm)
Side pier	LRB800	8000	442	17.2	2.7	3.9	1667
Middle pier	LRB1600	16,000	802	47.9	7.4	10.5	4724

5.2. Material Constitutive Model

The Scott–Kent–Park model is adopted for concrete in this study, as shown in Figure 11. K in the figure is the increase coefficient of concrete strength caused by restraint; f'_c is the compression strength of the concrete cylinder; ε_{\max} is the ultimate compressive strain of concrete. The reinforcement adopts the double straight line calculation model, ignoring the stress–strain relationship in the strengthening stage; see Figure 12, in which f'_y is the yield stress and ε_y is the yield strain. E_0 is the initial elastic modulus and b is the hardening ratio, with a value of 0.01. LRBs are used as the isolation bearings of the bridge, and the modified bilinear model is used for both; see Figure 13. In Figure 13, K_1 represents the stiffness before yield, K_2 represents the post-yielding stiffness, Q_d represents yield force, K_{eq} represents the equivalent horizontal stiffness, and u_1 represents yield displacement.

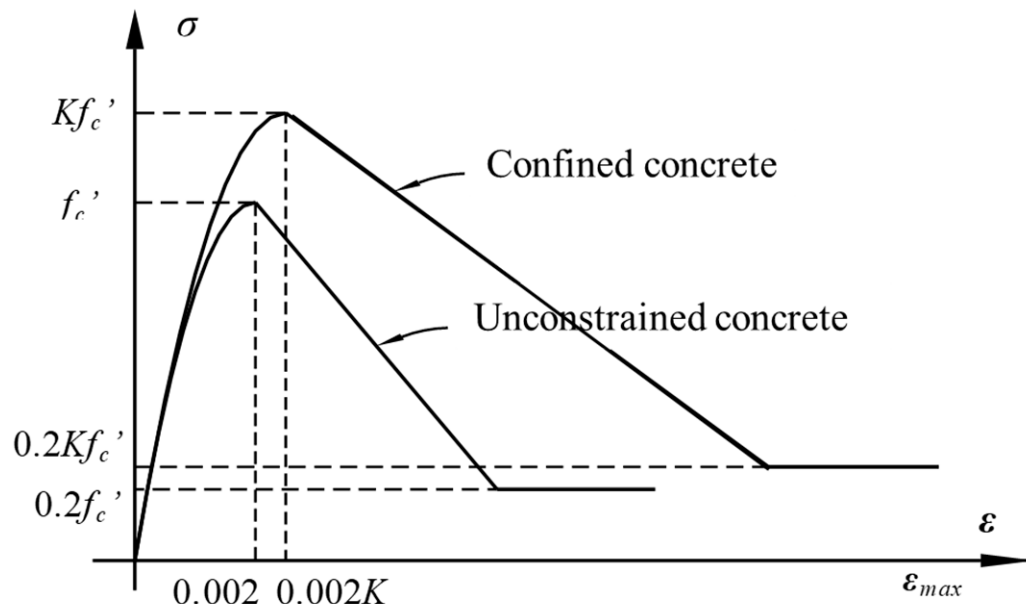


Figure 11. Kent Park constitutive model (concrete).

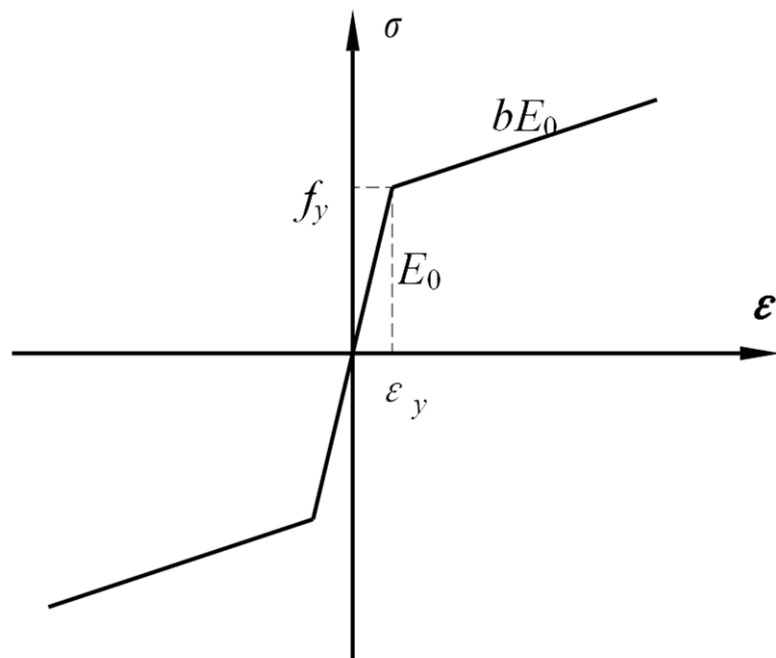


Figure 12. Bilinear model (rebar).

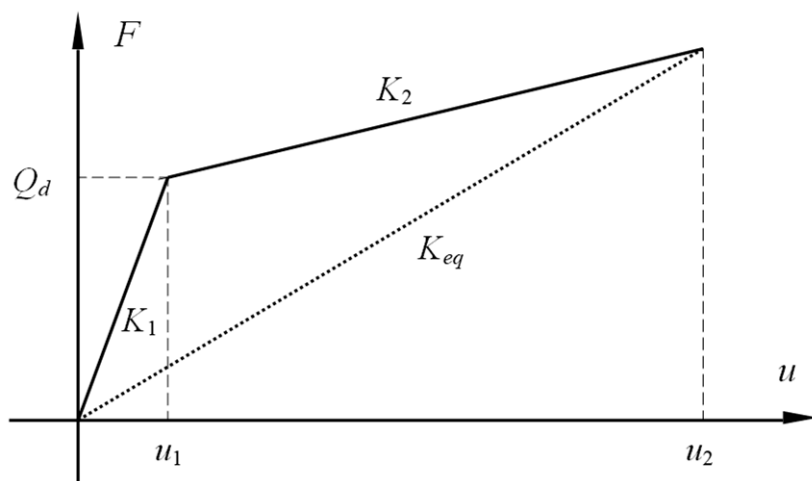


Figure 13. Modified bilinear model of LRBs.

5.3. Establishment of a Bridge Finite Model and the Selection of Ground Motion

The probability of damage of the main beam under an earthquake is small, and the pier and bearing are the most likely to damage under the earthquake. Therefore, the linear elastic beam–column element was used to imitate the working characteristics of the main beam when building the bridge structure model. The pier was the main stressed component, which bore the gravity of the superstructure and resisted the earthquake. At the same time, it dissipated the seismic energy through its own ductility to protect the main structure. The fiber plastic hinge element was used to simulate the pier. Considering that the ratio of the calculated height of the pier to the short side length of the rectangular section is less than 8, the influence of the P-Δ effect is ignored in the analysis [37]. The specific location of the plastic hinge is shown in Figure 14. And the blue dotted box is an enlarged picture of the content of the red dotted box in Figure 14. For the key component connecting the superstructure and substructure of the bridge–bridge isolation bearing, the simulation adopted a double rubber isolator element.

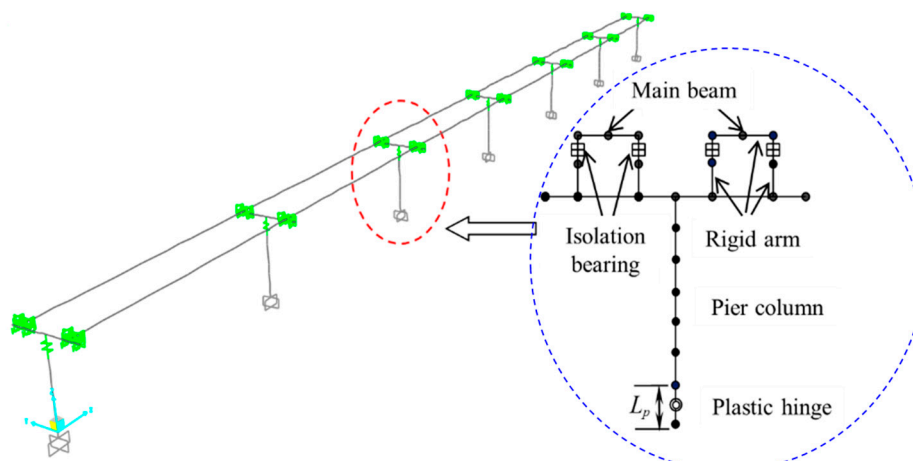


Figure 14. Schematic diagram of the bridge finite element model.

Both Chinese code [38] and American AASHTO specifications recommend using 3 or 7 seismic waves for seismic time history analysis, and the maximum response value is taken as the representative value when using 3 seismic waves, while the average response value is taken as the representative value when using seismic waves. In this paper, three seismic waves that meet the site conditions are selected from the latest seismic database of the Pacific seismic engineering research center (peer) [39], and the nonlinear dynamic time history analysis is carried out along the longitudinal input of the bridge. The selected ground motion acceleration response spectrum characteristics are shown in Figure 15, the ground motion information is shown in Table 7, and the normalized ground motion acceleration time history curve is shown in Figure 16.

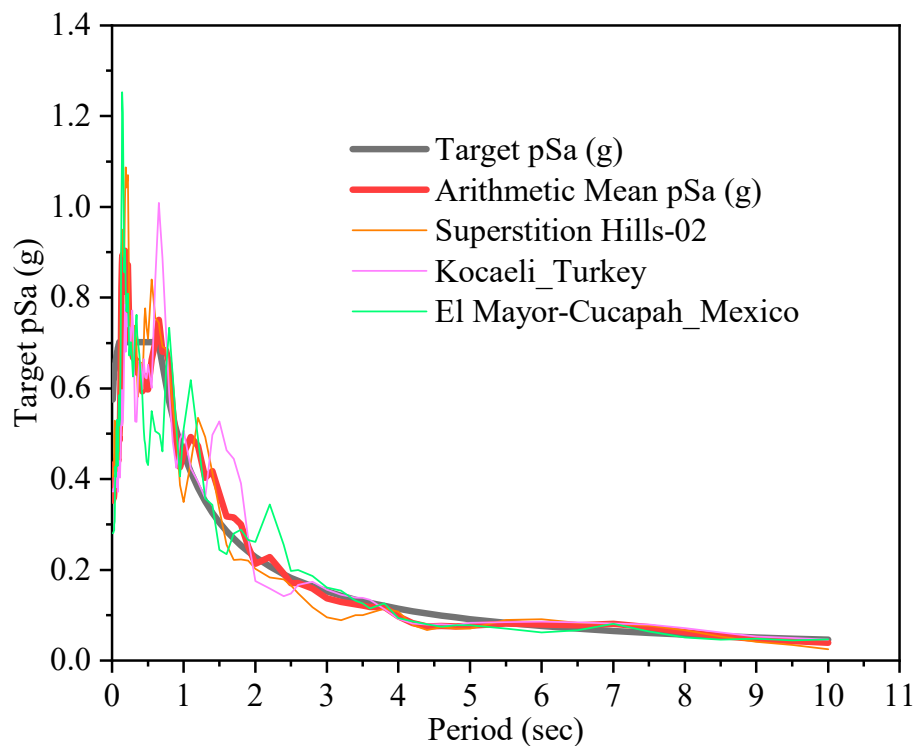


Figure 15. Characteristics of ground motion acceleration response spectrum.

Table 7. Seismic wave recording information.

Number	RSN	Earthquake Name	Year	Station Name	Magnitude	Rjb (km)	Vs30 (m·s ⁻¹)
1	721	Superstition Hills-02	1987	"El Centro Imp. Co. Cent"	6.54	18.2	192.05
2	1177	Kocaeli_Turkey	1999	"Zeytinburnu"	7.51	51.98	341.56
3	5832	El Mayor-Cucapah_Mexico	2010	"TAMAULIPAS"	7.2	25.32	242.05

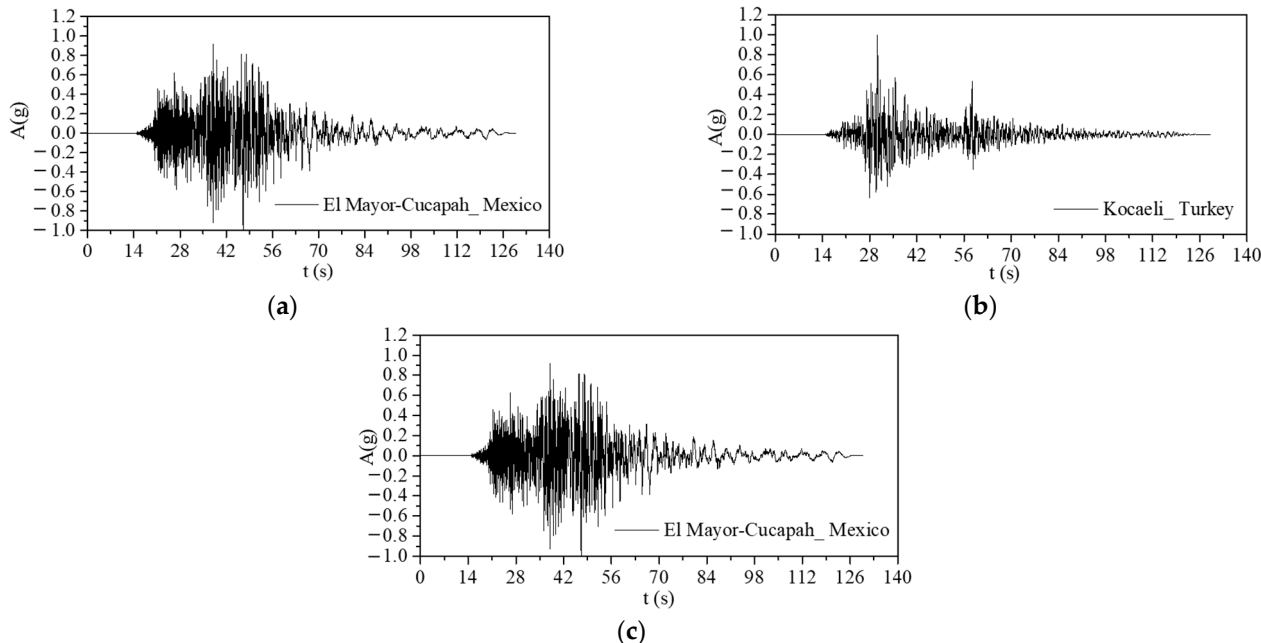


Figure 16. Three seismic wave acceleration time history curves. (a) Superstition Hills-02; (b) Kocaeli_Turkey; (c) E1 Mayor_Cucapah_Mexico.

5.4. Determination of LRB Time-Varying Parameters

According to the parameter information of LRBs given in Table 6, combined with the time-varying law formula of LRB horizontal stiffness and vertical stiffness under alternation of aging and seawater corrosion (see Formulas (1) and (2)) and the time-dependent law of LRB post-yield stiffness, yield stress, and pre-yield stiffness obtained by the research group, see Formula (6) to Formula (8) [40], the mechanical performance parameters of LRBs within 120 years of service are calculated, as shown in Table 8.

$$\frac{K_{d-LRB}(Y)}{K_{d-LRB}(0)} = 1.177 - 0.184 \times e^{-0.037 \times Y} \quad (6)$$

$$\frac{Q_{d-LRB}(Y)}{Q_{d-LRB}(0)} = 1 - 0.0004 \times Y \quad (7)$$

$$\frac{K_{1-LRB}(Y)}{K_{1-LRB}(0)} = \frac{K_{d-LRB}(Y)}{K_{d-LRB}(0)} = 1.177 - 0.184 \times e^{-0.037 \times Y} \quad (8)$$

where $K_{d-LRB}(Y)$, $Q_{d-LRB}(Y)$, and $K_{1-LRB}(Y)$ are, respectively, the post-yielding stiffness, yield stress, and pre-yield stiffness corresponding to the service time of Y years and $K_{d-LRB}(0)$, $Q_{d-LRB}(0)$, and $K_{1-LRB}(0)$ are the corresponding post-yield stiffness, yield stress, and pre-yield stiffness when the service time is 0 years.

Table 8. LRB time-varying parameters.

Service Time (Years)	0	30	60	90	120
Side pier LRB800	K_{eq} (kN/mm)	3.9	4.2707	4.4201	4.4756
	K_1 (kN/mm)	17.2	19.2014	19.9007	20.1311
	K_2 (kN/mm)	2.7	3.0142	3.1239	3.1601
	Q_y (kN)	442	431.8015	433.0988	434.4001
Middle pier LRB1600	K_{eq} (kN/mm)	10.5	11.4981	11.9002	12.0497
	K_1 (kN/mm)	47.9	53.4737	55.4211	56.0628
	K_2 (kN/mm)	7.4	8.2611	8.5619	8.6611
	Q_y (kN)	802	783.495	785.849	788.2101

In this study, SAP2000 was used to analyze the seismic performance of a bridge. The modal analysis of the finite-element model of an isolated continuous bridge was carried out, and the dynamic characteristics of the bridge structure were obtained. The structural period corresponding to the first six vibration modes at service times of 0, 30, 60, 90 and 120 years is drawn as Figure 17.

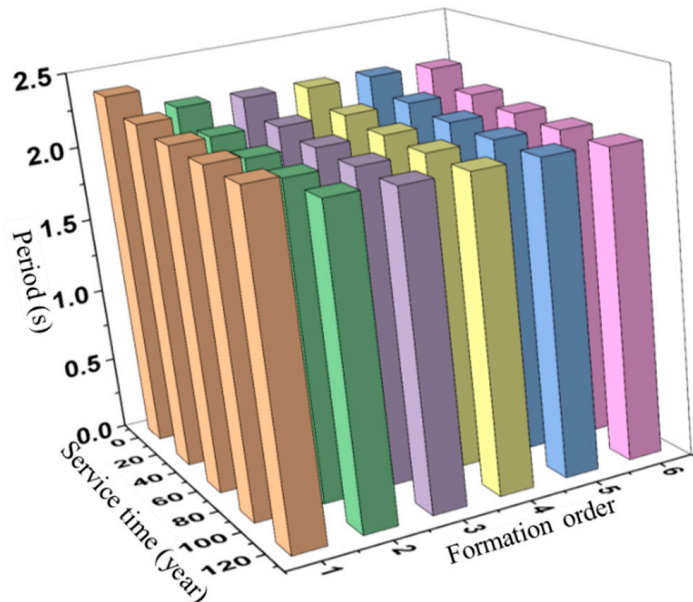


Figure 17. Variation of isolation structure period with service time and vibration mode under LRB deterioration.

Figure 17 indicates that, when different bearings are degraded, the isolation structure cycle of the first six vibration modes decreases with increasing service duration, which is because the horizontal equivalent stiffness of the bearing increases with increasing service time, and, after 120 years of service, the first vibration mode cycle of LRB degradation decreases by 5.6%. To sum up, the deterioration of bearings reduces the structural period, reduce the damping effect of the structure and deteriorating the earthquake resistance performance. Thus, it is necessary to analyze the influence of bridge bearing degradation on the seismic performance of the bridge.

5.5. Time-Varying Law of Earthquake Resistance Performance of an Offshore Isolated Bridge Considering the Performance Degradation of Isolation Bearings

Under the earthquake with a PGA of 0.443 g, the nonlinear time history analysis of the seismic isolated bridge was conducted, and the pier top displacement time history curve, pier bottom bending moment time history curve, pier bottom bending moment rotation angle curve, and isolation bearing hysteretic curve of the pier column under the single deterioration of an LRB are obtained. In view of the length problem, only the results of the displacement time history response of 2# pier top and moment time history response of the pier bottom at different service time points under the action of Superstition Hills-02 wave are given, as shown in Figures 15–18. Additionally the time history curves of structural response after 0, 60, and 120 years of deterioration for the LRB are given in Figures 18–20.

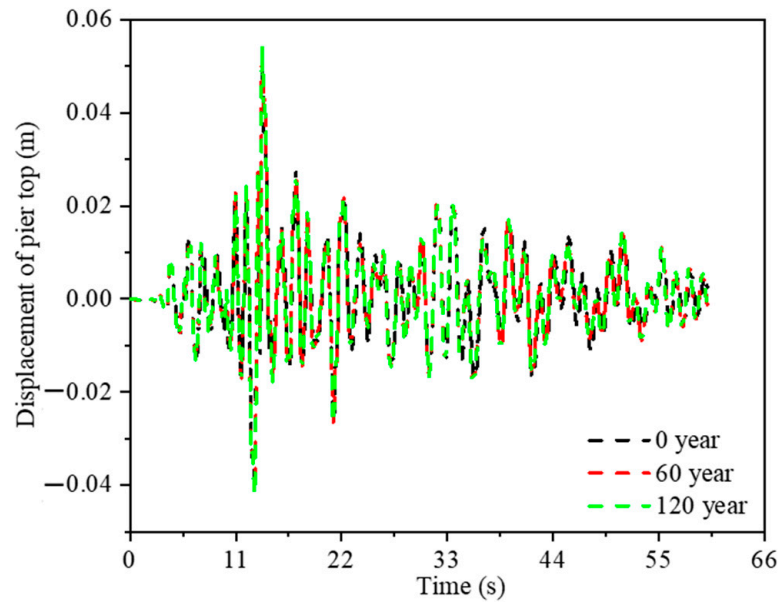


Figure 18. Time history curve of 2# pier top displacement under LRB performance degradation.

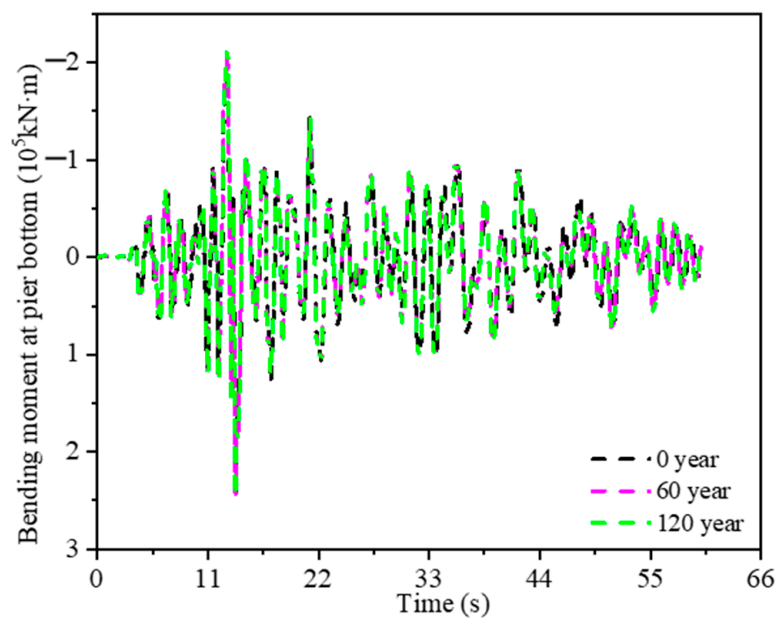


Figure 19. Time history curve of 2# pier bottom bending moment under LRB degradation.

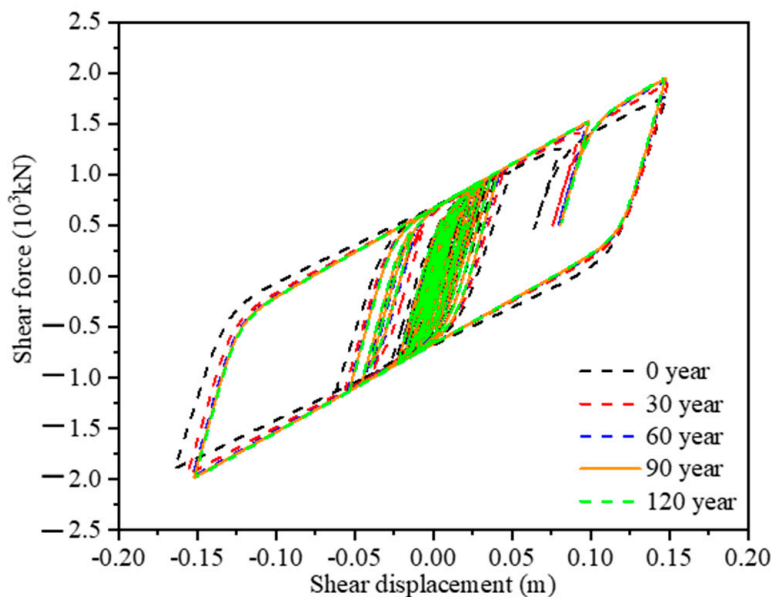


Figure 20. Comparison of the hysteresis curves of the LRB at different deterioration time points.

Figures 18 and 19 show that, considering the deterioration of bearing performance, there is no significant difference between the top displacement and pier bottom bending moment of the bridge at 60 and 120 years of service at the initial stage of the earthquake and the value at the initial 0 year. At this time, the bearing has not yielded. With the continuous ground motion, both the pier displacement and the pier bottom bending gradually increase, and the bridge isolation bearing may reach the yield point and have nonlinear deformation. From 60 to 120 years of bearing deterioration, the top displacement and pier bottom bending increase with increasing deterioration time, which is due to the increase of bridge bearing stiffness, the decrease of the isolation effect, and the increase of structural response.

Figure 20 indicates that the yield stress and post-yielding stiffness of the LRB becomes larger with the increase of deterioration time, while the ultimate displacement becomes smaller. Additionally, the LRB's hysteretic loop area decreases with deterioration time, which leads to the decrease of the energy dissipation capacity of the bearing and increases the earthquake response of the main body of the isolated bridge structure. Especially when it has been in service for 30 years, the shear force of the bearing increases obviously and the shear displacement decreases obviously.

Figure 21 states that the isolation bearing has a certain impact on the hysteretic curve of the pier column. With the increase of service time, the pier–column bending moment increases slightly, while the angular displacement increases significantly. This is because the deterioration of the bending increases its yield stiffness and yield force, and the energy dissipation of the bearing decreases, resulting in the increase of angular displacement of pier bottom.

The absolute value of the ratio between the maximum structural response when in service for Y years and the response when in service for 0 years is defined as the maximum value ratio of structural response. The variation law of the maximum value ratio of structural response with the service time is shown in Figure 22.

Figure 22 states clearly that the maximum displacement of the pier top increases with the increase of service time under the action of 0.443 g ground motion. After 120 years of service, the maximum displacement increase amplitude of the pier top is 14.2% under the condition of LRB deterioration. Additionally, the deterioration of the isolation bearing has little effect on the maximum bending moment at the pier bottom, and after servicing for 120 years, the maximum bending moment at the pier bottom increases by 6.6% under the condition of LRB deterioration. The rubber bearing's maximum displacement decreases with increasing service duration when considering that the bearing deteriorates alone. The

bearing's maximum displacement reduces by 9.1% after it is in service for 120 years. This indicates that the deformation and energy dissipation capacity of the bearing decreases, the isolation effect decreases, the response of the main structure increases, and the protection effect of the bearing on the main structure decreases.

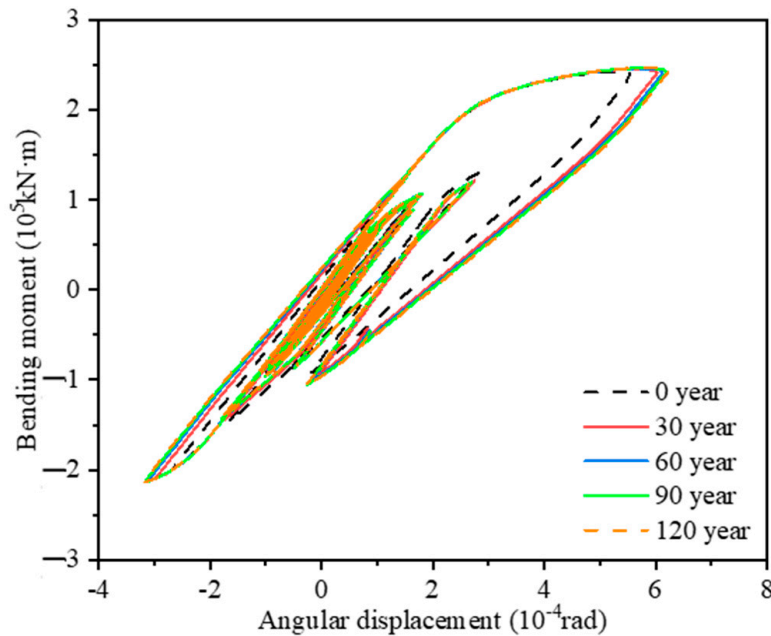


Figure 21. Bending moment–angle curve of pier bottom under LRB deterioration.

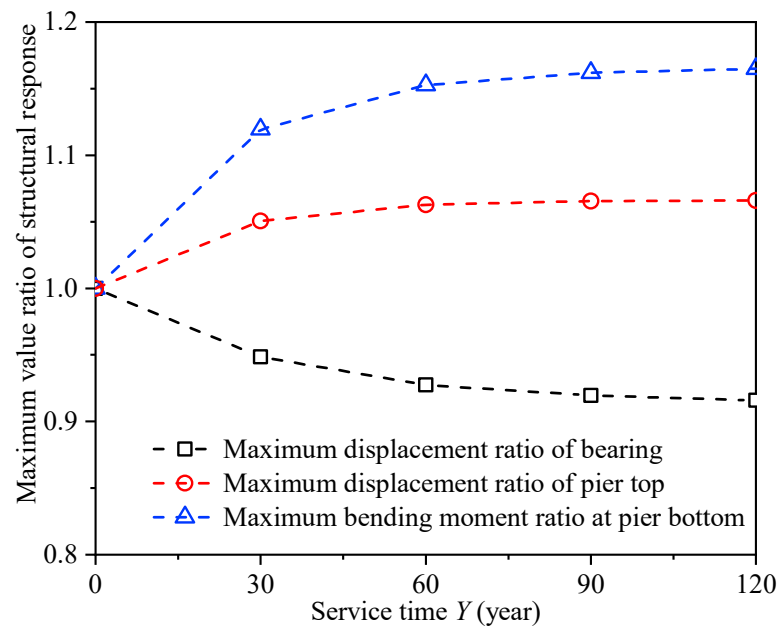


Figure 22. Maximum value ratio of structural response.

To sum up, the finite element analysis of the offshore isolation bridge is carried out by SAP2000 in this study. The pier top displacement time history curve, pier bottom bending moment time history curve, pier bottom bending moment rotation angle curve, and isolation bearing hysteretic curve of the pier column under the single deterioration of LRB are obtained; see Figures 18–22. The results show that the deterioration of lead rubber isolation bearing has a great influence on the seismic performance of the offshore isolation

bridge. In the seismic performance analysis of the offshore isolation bridge, not only the influence of concrete materials such as the pier column but also the influence of isolation bearing deterioration should be considered.

6. Summary and Conclusions

The aim of this study is to investigate the influence of the alternation of aging and seawater corrosion on the performance deterioration law of lead rubber bearings used in offshore bridges. The effect of LRB deterioration on the earthquake resistant behavior of an offshore isolation bridge was also studied in this paper. Thus, a 120-day alternating aging–seawater corrosion test on lead rubber bearings and rubber material was carried out, and the time-dependent law of the LRB basic properties and rubber material constitutive parameters were also obtained in this paper. Then, rubber material parameters obtained were substituted into the finite-element model of LRBs to simulate the horizontal and vertical stiffness at different test time points, and the fitting results, simulation results, and test results of those were compared. Finally, the time-variable law of the seismic performance of offshore bridge structures was also analyzed, which was based on the time-variable law of the horizontal and vertical stiffness ratio of LRBs during the 120-year service period, the time-dependent law of the seismic performance of offshore bridge structures was analyzed. The results state that:

The horizontal stiffness and vertical stiffness of LRBs increase with increasing aging and seawater corrosion alternation time. After 120 days of testing, the increase of the two was 16.3% and 24.3%, respectively; the rubber material parameter C_{10} of LRBs increases with the test time, while parameter C_{01} decreases with the increase of test time, and the material parameters change greatly. The time-dependent law of the material parameters of LRBs is revealed in Formulas (4) and (5); the simulation results are generally consistent with the fitting values of the corresponding test results, which verifies the rationality of the deterioration law of horizontal stiffness and vertical stiffness with the alternation of aging and seawater corrosion test duration; after servicing for 120 years, the variation amplitudes of the maximum pier top displacement, the maximum pier bottom bending, and the maximum bearing displacement of the bridge structure are 14.2%, 6.6%, and 9.1% respectively, under the condition of LRB deterioration. To sum up, the alternation of aging and seawater corrosion plays a significant role in LRB basic performance, and the influence of LRB degradation on the seismic behavior of offshore isolated bridges cannot be ignored. In the next study, we will carry out a comparative study on the performance deterioration of different kinds of rubber isolations and its impact on the earthquake resistance behavior of bridge structures, and propose solutions to bearing performance degradation.

Author Contributions: Conceptualization, Y.L. and Y.M.; methodology, Y.L. and Y.M.; software, Y.L. and R.L.; validation, Y.L., Y.M. and R.L.; formal analysis, Y.M. and R.L.; investigation, Y.M., G.Z. and R.L.; resources, Y.M. and G.Z.; data curation, Y.L., Y.M. and G.Z.; writing—original draft preparation, Y.L. and R.L.; writing—review and editing, Y.L., Y.M. and G.Z.; visualization, Y.L., Y.M., G.Z. and R.L.; supervision, Y.M. and G.Z.; project administration, Y.M. and G.Z.; funding acquisition, Y.M. and G.Z. All authors have read and agreed to the published version of the manuscript.

Funding: This work was supported by the National Natural Science Foundation of China (52078150, 51878196), National Key Research and Development Plan (2019YFE0112500), China. Guangdong Key Laboratory of Earthquake Engineering & Applied Technique (2020B1212060071).

Data Availability Statement: Not applicable.

Acknowledgments: The authors gratefully acknowledge the financial support of this work by the Guangzhou University. They also acknowledge the Earthquake Engineering Research & Test Center, Guangdong Key Laboratory of Earthquake Engineering & Applied Technique and Key Laboratory of Earthquake Resistance, Earthquake Mitigation and Structural Safety, Ministry of Education.

Conflicts of Interest: The authors declare no conflict interest.

References

- Shen, C.; Zhou, F.; Wen, H.; Ma, Y.; Chen, Y. Test study on mechanical property of different type of isolators for bridge. *China Civ. Eng. J.* **2012**, *45*, 233–237.
- Zhuang, X.; Shen, C.; Jin, J. Experimental study on mechanical property of high damping rubber bearing for bridge. *Earthq. Eng. Eng. Vib.* **2006**, *26*, 208–212.
- Akihiro, M. Evaluation for Mechanical Properties of Laminated Rubber Bearings Using Finite Element Analysis. *J. Press. Vessel. Technol.* **2004**, *126*, 134–140.
- Xu, B.; Tang, J.-X. Experimental Studies on Durability of base isolation of using Laminated Rubber Bearings. *Eathq. Resist. Eng.* **1995**, *4*, 41–44.
- Itoh, Y.; Gu, H.S. Prediction of aging characteristics in natural rubber bearings Used in Bridges. *J. Bridge Eng.* **2009**, *14*, 122–128. [[CrossRef](#)]
- Itoh, Y.; Gu, H.; Satoh, K.; Kutsuna, Y. Experimental investigation on ageing behaviors of rubbers used for bridge bearings. *Doboku Gakkai Ronbunshuu A* **2006**, *62*, 176–190. [[CrossRef](#)]
- Itoh, Y.; Yazawa, A.; Kitagawa, T. Study on environmental durability of rubber bearing for bridges. *Int. Assoc. Bridge Struct. Eng.* **2002**, *86*, 137–143.
- Itoh, Y.; Gu, H.; Satoh, K.; Yamamoto, Y. Long-term deterioration of high damping rubber bridge bearing. *Doboku Gakkai Ronbunshuu A* **2006**, *62*, 595–607. [[CrossRef](#)]
- Gu, H.S.; Itoh, Y. Ageing effects on high damping bridge rubber bearing. In Proceedings of the 6th Asia-Pacific Structural Engineering and Construction Conference (APSEC 2006), Kuala Lumpur, Malaysia, 5–6 September 2006.
- Wang, J.; Zhang, Z.; Li, Z. Experimental research on the vertical pressure dependence about shear properties of high damping rubber bearing. *J. Railw. Eng. Soc.* **2017**, *34*, 117.
- Wang, J.; Wei, X.; Zhuo, L.; Zheng, Z. Experimental study on vertical pressure dependency about shear properties of lead rubber bearing. *Earthq. Eng. Eng. Dyn.* **2016**, *36*, 200–206.
- Li, Y.; Zong, Z.; Huang, X.; Xia, J.; Liu, L. Experimental study on mechanical properties of high damping rubber bearing model. *IOP Conf. Ser. Earth Environ. Sci.* **2017**, *61*, 1–6. [[CrossRef](#)]
- Park, J.; Choun, Y.; Kim, M.K.; Hahm, D. Revaluation of the aging property modification factor of lead rubber bearings based on accelerated aging tests and finite element analysis. *Nucl. Eng. Des.* **2019**, *347*, 59–66. [[CrossRef](#)]
- Kalpakidis, V.I.; Constantinou, M.C. Effects of heating on the behavior of lead-rubber bearings, II: Verification of Theory. *J. Struct. Eng.* **2009**, *135*, 1450–1461. [[CrossRef](#)]
- Kalpakidis, V.I.; Constantinou, M.C. Effects of heating on the behavior of lead-rubber bearings. I: Theory. *J. Struct. Eng.* **2009**, *135*, 1440–1449. [[CrossRef](#)]
- Takenaka, Y. Experimental study on heat-mechanics interaction behavior of laminated rubber bearings. *J. Struct. Constr. Eng.* **2009**, *74*, 2245–2253. [[CrossRef](#)]
- Biondini, F.; Camnasio, E.; Palermo, A. Lifetime seismic performance of concrete bridges exposed to corrosion. *Struct. Infrastruct. Eng.* **2014**, *10*, 880–900. [[CrossRef](#)]
- Alipou, A.; Shafei, B.; Shinotsuka, M. Performance Evaluation of Deteriorating Highway Bridges Located in High Seismic Areas. *J. Bridge Eng.* **2011**, *16*, 597–611. [[CrossRef](#)]
- Kobayashi, K. The seismic behavior of RC member suffering from chloride induced corrosion. In Proceedings of the 2nd Fib International Congress, Naples, Italy, 5–8 June 2006.
- Choe, D.E.; Gardoni, P.; Rosowsky, D.; Haukaas, T. Probabilistic capacity models and seismic fragility estimates for RC columns subject to corrosion. *Reliab. Eng. Syst. Saf.* **2008**, *93*, 383–393. [[CrossRef](#)]
- Ghosh, J.; Padgett, J.E. Aging Considerations in the Development of Time-Dependent Seismic Fragility Curves. *J. Struct. Eng.* **2010**, *136*, 1497–1511. [[CrossRef](#)]
- Zhao, G.; Ma, Y.; Jian, T.; Su, L.; Zhou, F. Effects of performance deterioration of friction pendulum bearings on seismic behavior of Hong Kong-Zhuhai-Macao isolated bridges in life-cycle period. *China J. Highw. Transp.* **2016**, *29*, 10–16. (In Chinese)
- Chen, J.-J.; Ma, Y.; Jin, H.; Guifeng, Z. Time-dependent Seismic Fragility Analysis of Offshore Bridges Based on Aging Time-dependent Law of Rubber Bearings. *Sci. Technol. Eng.* **2020**, *20*, 3699–3706.
- Farhangi, V.; Karakouzian, M. Effect of Fiber Reinforced Polymer Tubes Filled with Recycled Materials and Concrete on Structural Capacity of Pile Foundations. *Appl. Sci.* **2020**, *10*, 1554. [[CrossRef](#)]
- Mitoulis, S.; Titirla, M.; Tegos, I. Design of bridges utilizing a novel earthquake resistant abutment with high capacity wing walls. *Eng. Struct.* **2014**, *66*, 35–44. [[CrossRef](#)]
- Nutt, R.V.; Mayes, R.L. Comparison of typical bridge columns seismically designed with and without abutment participation using AASHTO division I-A and proposed AASHTO LRFD provisions. Task F3-1(a). In *AASHTO LRFD Bridge Design Specifications*; AASHTO: New York, NY, USA, 2000.
- Ma, Y.; Li, Y.; Zhao, G.; Khaloo, A. Experimental research on the time-varying law of performance for natural rubber laminated subjected to alternating of aging and seawater erosions. *Eng. Struct.* **2019**, *17*, 159–171. [[CrossRef](#)]
- Li, Y.; Ma, Y.; Zhao, G.; Zhou, F. Experimental study on the property deterioration of rubber material used as natural rubber bearing under seawater wet-dry cycles. *J. Vib. Shock* **2019**, *38*, 146–152.

29. Li, Y.; Ma, Y.; Zhao, G.; Zhou, F. Experimental study on the effect of alternating ageing and sea corrosion on laminated natural rubber bearing's tension-shear property. *J. Rubber Res.* **2020**, *23*, 151–161. [[CrossRef](#)]
30. Zhao, G.; Ma, Y.; Li, Y.; Luo, J.; Du, C. Development of a modified mooney-rivlin constitutive model for rubber to investigate the effects of aging and marine corrosion on seismic isolated bearings. *Earthq. Eng. Eng. Vib.* **2017**, *16*, 815–826. [[CrossRef](#)]
31. ISO 22762-1:2005; Elastomeric SeismicProtection Isolators—Part 1: Test Methods, MOD. ISO: Geneva, Switzerland, 2005.
32. ISO 22762-2:2005; Elastomeric SeismicProtection Isolators—Part 2: Applications for Bridges—Specifications, MOD. ISO: Geneva, Switzerland, 2005.
33. Li, Y.; Ma, Y.; Luo, J.; Zhao, G. The effect of aging on the material constant of the rubber isolator's constitutive model Mooney-Rivlin. *J. Vib. Shock.* **2016**, *35*, 164–169. (In Chinese)
34. Li, Y.; Zhao, G.; Ma, Y.; Liu, R. Effect of alternation of aging and seawater erosion on properties of rubber material used in lead rubber bearing. *J. Renew.* **2022**, *10*, 1641–1658. [[CrossRef](#)]
35. Liu, R.; Ma, Y.; Zhao, G.; Li, Y.; Zheng, N. Influence of freeze-thaw cycles and aging on the horizontal mechanical properties of high damping rubber bearings. *J. Rubber Res.* **2022**, *25*, 69–77. [[CrossRef](#)]
36. Huang, J.; Xie, G.; Liu, Z. Finite element analysis of hyperelastic rubber material based on Mooney-Rivlin model and Yeoh model. *China Rubber Ind.* **2008**, *8*, 467–471. (In Chinese)
37. Ye, A.; Guan, Z. *Seismic Design of Bridges*, 2nd ed.; China Communications Press: Beijing, China, 2011.
38. Liu, C. *Seismic Response and Seismic Performance Analysis of Bridge Structures*, 1st ed.; China Construction Industry Press: Beijing, China, 2009.
39. CJJ 166-2011; Code for Seismic Design of Urban Bridges. Tongji University: Shanghai, China, 2011.
40. Li, Y. Study on Bidge Isolation Bearings Performance Deterioration Law under Aging-Seawater Erosion Alternation. Ph.D. Thesis, Guangzhou University, Guangzhou, China, 2021.

Disclaimer/Publisher's Note: The statements, opinions and data contained in all publications are solely those of the individual author(s) and contributor(s) and not of MDPI and/or the editor(s). MDPI and/or the editor(s) disclaim responsibility for any injury to people or property resulting from any ideas, methods, instructions or products referred to in the content.